

Probing “long-range” neutrino-mediated forces with atomic and nuclear spectroscopy

Yevgeny V. Stadnik

Johannes Gutenberg University of Mainz, 55128 Mainz, Germany

(Dated: August 15, 2022)

The exchange of a pair of low-mass neutrinos between electrons, protons and neutrons produces a “long-range” $1/r^5$ potential, which can be sought for in phenomena originating on the atomic and nuclear scales. We calculate the effects of neutrino-pair exchange on transition and binding energies in atoms and nuclei. In the case of atomic s -wave states, there is a particularly large enhancement of the induced energy shifts due to the lack of a centrifugal barrier and the highly singular nature of the neutrino-mediated potential. We derive limits on neutrino-mediated forces from measurements of the deuteron binding energy and transition energies in positronium, muonium, hydrogen and deuterium, as well as isotope-shift measurements in calcium ions. Our limits improve on existing constraints on neutrino-mediated forces from experiments that search for new macroscopic forces by 18 orders of magnitude. Future spectroscopy experiments have the potential to probe long-range forces mediated by the exchange of pairs of standard-model neutrinos and other weakly-charged particles.

PACS numbers: 32.30.-r, 32.10.Bi, 21.10.Dr, 13.15.+g

Introduction. — The neutrino is a neutral low-mass fermion that was originally proposed by Wolfgang Pauli in order to explain the observed spectrum of beta-decay processes. In the standard model of particle physics, there are three flavours of neutrinos which interact with other particles via the weak interaction. Current experimental efforts to study the properties of neutrinos are largely based around the detection of neutrinos from laboratory and astrophysical sources, see, e.g., the review [1] and references therein.

The exchange of a pair of neutrinos between two particles is predicted to mediate a long-range force between the particles (see, e.g., Refs. [2, 3] and references therein for a historical overview of this problem, which dates back to the 1930’s). In Ref. [3] (see also [4–8]), the long-range part of the potential due to the exchange of a pair of massless neutrinos between two particles was calculated and found to scale as $\propto 1/r^5$. The $1/r^5$ neutrino-mediated potential induces a feeble $1/r^6$ force which is far too small to detect with current experiments that search for new macroscopic forces [9–13].

In the present work, we consider the different approach of searching for effects associated with the neutrino-mediated $1/r^5$ potential on atomic and nuclear length scales. Compared to a macroscopic length scale of $L = 1$ mm, the magnitude of a $1/r^5$ potential between two point-like particles is enhanced by the factors $(L/a_B)^5 \sim 10^{36}$ and $(L/r_0)^5 \sim 10^{60}$ on atomic and nuclear length scales, respectively, where $a_B \approx 5.29 \times 10^{-11}$ m is the atomic Bohr radius and $r_0 \approx 1.2 \times 10^{-15}$ m is a distance parameter related to the internucleon separation.

In the case of atomic s -wave states (states with orbital angular momentum $l = 0$), there is an additional enhancement due to the lack of a centrifugal barrier and the highly singular nature of the $1/r^5$ potential. As the simplest example, the radial part of the non-relativistic $1s$ hydrogen wavefunction scales as $R_{1s}(r) \propto$

$r^0/a_B^{3/2}$ at small distances, meaning that the integral $\int_{r_c}^{\infty} r^2 [R_{1s}(r)]^2 / r^5 dr$ diverges like $\propto 1/r_c^2$ for a point-like nucleus ($r_c = 0$). In the physical hydrogen atom with a finite-size nucleus ($r_c \sim r_0$), this integral is finite and scales parametrically like $\sim 1/(a_B^3 r_0^2)$, which is enhanced compared to the characteristic $\sim 1/a_B^5$ scaling in atomic states of higher orbital angular momentum by the factor $(a_B/r_0)^2 \sim 10^9$.

Measurements of transition and binding energies in atoms and nuclei provide a powerful way of probing neutrino-mediated forces, since energy differences (or equivalently frequencies) are among the most accurately measurable physical quantities. In particular, current state-of-the-art atomic and ionic clocks operating on optical transitions have already demonstrated a fractional precision at the level of $\sim 10^{-18}$ [14–19]. In the present work, we explore the possibility of leveraging these phenomenal levels of precision to search for neutrino-mediated forces.

Potential induced by the exchange of a pair of low-mass neutrinos. — In this work, we consider phenomena in atoms and nuclei. The potential mediated by the exchange of a pair of neutrinos of non-zero mass m_ν is long-range in an atom, if the size of the atom is much smaller than the Yukawa range parameter associated with the pair of neutrinos, $\lambda = 1/(2m_\nu) \gg R_{\text{atom}}$. Beta-decay experiments directly constrain the electron-antineutrino mass to be $m_{\bar{\nu}_e} \lesssim 2$ eV [20, 21], while cosmological observations give model-dependent constraints on the sum of the three different neutrino masses at a comparable level [1]. This implies a Yukawa range parameter of $\lambda \gtrsim 10^{-7}$ m $\gg R_{\text{atom}}$, and so we can treat the neutrino-mediated potential as being long-range.

The long-range part of the potential due to the exchange of a pair of low-mass neutrinos between two

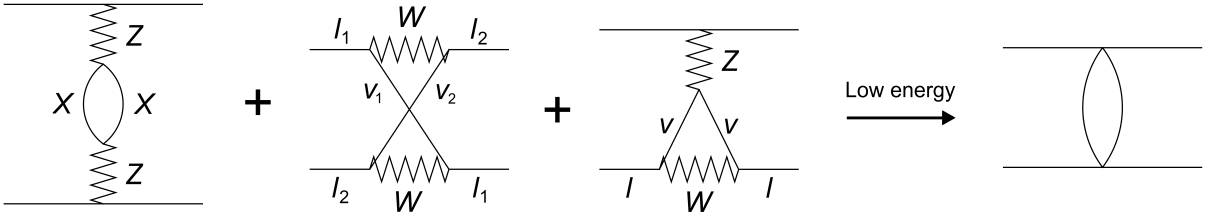


FIG. 1. Weak-neutral-current and weak-charged-current processes that give rise to a long-range $1/r^5$ potential between two fermions. X denotes a weakly-charged species, l denotes a charged lepton and ν denotes the corresponding neutrino species.

fermions reads as follows [3–5]:

$$\begin{aligned} V_\nu(\mathbf{r}) &= \frac{G_F^2}{4\pi^3 r^5} \left\{ a_1 a_2 - b_1 b_2 \left[\frac{3}{2} \boldsymbol{\sigma}_1 \cdot \boldsymbol{\sigma}_2 - \frac{5}{2} (\boldsymbol{\sigma}_1 \cdot \hat{\mathbf{r}}) (\boldsymbol{\sigma}_2 \cdot \hat{\mathbf{r}}) \right] \right\} \\ &= \frac{G_F^2}{4\pi^3 r^5} \left\{ a_1 a_2 - \frac{2}{3} b_1 b_2 \boldsymbol{\sigma}_1 \cdot \boldsymbol{\sigma}_2 \right. \\ &\quad \left. - \frac{5}{6} b_1 b_2 [\boldsymbol{\sigma}_1 \cdot \boldsymbol{\sigma}_2 - 3 (\boldsymbol{\sigma}_1 \cdot \hat{\mathbf{r}}) (\boldsymbol{\sigma}_2 \cdot \hat{\mathbf{r}})] \right\}, \quad (1) \end{aligned}$$

where $G_F \approx 1.166 \times 10^{-5} \text{ GeV}^{-2}$ is the Fermi constant of the weak interaction, r is the distance between the two fermions, $\boldsymbol{\sigma}_1$ and $\boldsymbol{\sigma}_2$ are the Pauli spin matrix vectors of fermions 1 and 2, and $\hat{\mathbf{r}}$ is the unit vector directed between the two fermions. In the present work, we focus mainly on systems in $l = 0$ states, which are described by spherically symmetric wavefunctions. For such states, the expectation value of the rank-2 tensor part in (1) vanishes: $\langle [\boldsymbol{\sigma}_1 \cdot \boldsymbol{\sigma}_2 - 3 (\boldsymbol{\sigma}_1 \cdot \hat{\mathbf{r}}) (\boldsymbol{\sigma}_2 \cdot \hat{\mathbf{r}})] / r^5 \rangle_{l=0} = 0$.

The species-dependent parameters a_i and b_i in Eq. (1) are determined by several processes involving weak neutral and charged currents (see Fig. 1). For a single neutrino species, charged leptons receive contributions from both the weak neutral and charged currents: $a_l^{(1)} = 1 + g_l^V = 1/2 + 2 \sin^2(\theta_W)$ and $b_l^{(1)} = 1 + g_l^A = 1/2$, with $\sin^2(\theta_W) \approx 0.24$ [22], while nucleons receive a contribution solely from the weak neutral currents: $a_n^{(1)} = -1/2$, $a_p^{(1)} = 1/2 - 2 \sin^2(\theta_W)$, $b_n^{(1)} = -g_A/2$, and $b_p^{(1)} = g_A/2$, with $g_A \approx 1.27$. The nucleons and charged leptons also receive contributions from the other two neutrino species, due purely to the weak-neutral-current processes, with each neutrino species contributing the amount $a_i^{(2)} = g_i^V$, $b_i^{(2)} = g_i^A$, $a_N^{(2)} = a_N^{(1)}$ and $b_N^{(2)} = b_N^{(1)}$.

Furthermore, there are additional contributions from other weakly-charged species of mass m via the purely weak-neutral-current process in Fig. 1, when the dominant effects of the potential (1) arise at length scales $L \ll 1/(2m)$. The effects of these weakly-charged species are analogous to the effects of neutrino species in the weak-neutral-current channel, except for an overall numerical constant, which is given by $2[(g_l^V)^2 + (g_l^A)^2] \approx 0.501$ for a charged lepton species, $2[(g_u^V)^2 + (g_u^A)^2] \approx 0.565$ for an up-type quark species, and $2[(g_d^V)^2 + (g_d^A)^2] \approx 0.731$ for a down-type quark species.

Altogether, the combinations of species-dependent parameters in Eq. (1) therefore have the following effective

values:

$$a_1 a_2 \rightarrow a_1^{(1)} a_2^{(1)} + (N_{\text{eff}} - 1) a_1^{(2)} a_2^{(2)}, \quad (2)$$

$$b_1 b_2 \rightarrow b_1^{(1)} b_2^{(1)} + (N_{\text{eff}} - 1) b_1^{(2)} b_2^{(2)}. \quad (3)$$

In systems where the dominant effects of (1) arise on the atomic length scale, the main contributions are from the species ν_e , ν_μ and ν_τ , giving $N_{\text{eff}} \approx 3$. In systems where the dominant effects of (1) arise on the nuclear length scale, the main contributions are from the species ν_e , ν_μ , ν_τ , e , u and d , giving $N_{\text{eff}} \approx 4.80$. Finally, in systems where the dominant effects of (1) arise on a length scale of the order of the Compton wavelength of the Z boson, the main contributions are from the species ν_e , ν_μ , ν_τ , e , μ , τ , u , c , d , s and b , giving $N_{\text{eff}} \approx 7.83$. The overall sign of the potential (1) is reversed when one of the two fermions is replaced by its antiparticle.

Deuteron binding energy. — We start with nuclei, which are the smallest systems that can be probed by spectroscopic methods. For concreteness, we consider the simplest and best-studied nucleus, namely the deuteron, which is a bound state of a proton and a neutron in the 3S_1 state (with a small admixture of the 3D_1 state, which can be neglected in the first approximation). We employ the simple model of a spherical potential well with an infinitely repulsive inner hard core, in which the potential between the two nucleons takes the following form:

$$V_{\text{nucl}}(r) = \begin{cases} +\infty & \text{for } r < r_1, \\ -|V_0| & \text{for } r_1 < r < r_2, \\ 0 & \text{for } r > r_2, \end{cases} \quad (4)$$

where $|V_0|$ is the depth of the spherical potential well. For our estimates, we assume the values $r_1 = 0.5 \text{ fm}$ and $r_2 = 2.5 \text{ fm}$.

The radial wavefunction solutions of the potential (4) for an s -wave state are given by:

$$R_s(r) = \begin{cases} 0 & \text{for } r \leq r_1, \\ C_1 j_0(kr) + C_2 n_0(kr) & \text{for } r_1 \leq r \leq r_2, \\ C_3 h_0^{(1)}(i\kappa r) & \text{for } r \geq r_2, \end{cases} \quad (5)$$

where j is the spherical Bessel function of the first kind, n is the spherical Bessel function of the second kind, $h^{(1)}$ is the spherical Hankel function of the first kind, $k = \sqrt{2\mu(|V_0| - E_B)}$ and $\kappa = \sqrt{2\mu E_B}$, with $\mu = m_n m_p / (m_n + m_p) \approx 0.47 \text{ GeV}$ being the deuteron

reduced mass and $E_B \approx 2.2$ MeV the deuteron binding energy. Requiring the continuity of R_s at $r = r_1$ and the continuity of both R_s and dR_s/dr at $r = r_2$, we determine that $|V_0| \approx 36$ MeV. The normalisation condition $\int_0^\infty r^2 |R_s(r)|^2 dr = 1$ then fixes the normalisation constants in Eq. (5) to be $C_1 \approx 0.46 \text{ fm}^{-3/2}$, $C_2 \approx 0.22 \text{ fm}^{-3/2}$, and $C_3 \approx -0.22 \text{ fm}^{-3/2}$.

Using the wavefunction in Eq. (5), we calculate the expectation value of the $1/r^5$ operator for the deuteron bound state to be:

$$\left\langle {}^3S_1 \left| \frac{1}{r^5} \right| {}^3S_1 \right\rangle \approx 0.060 \text{ fm}^{-5}. \quad (6)$$

Using the result (6), we determine the change in the deuteron binding energy due to the neutrino-mediated potential (1) to be:

$$\delta E_B({}^3S_1) \approx -\frac{G_F^2}{4\pi^3} \left(a_n a_p - \frac{2}{3} b_n b_p \right) \times 0.060 \text{ fm}^{-5}. \quad (7)$$

Comparing the measured [24] and predicted [25, 26] values of the deuteron binding energy:

$$E_B^{\text{exp}} = 2.2245663(4) \text{ MeV}, \quad (8)$$

$$E_B^{\text{theor}} = 2.22457(1) \text{ MeV}, \quad (9)$$

and using expressions (7), (2) and (3), we place the following constraints on the neutrino-mediated potential in Eq. (1):

$$G_{\text{eff}}^2 \lesssim 5.8 \times 10^8 G_F^2. \quad (10)$$

Spectroscopy of simple atoms. — We next look at simple atoms consisting of only two bodies. Since we will only consider simple atoms with relatively light nuclei ($Z \sim 1$), it is sufficient to work in the non-relativistic framework. As explained in the introduction, there is a very large enhancement of the effects of the neutrino-mediated potential (1) on atomic s -wave states.

Using the non-relativistic form of the wavefunctions for a hydrogen-like system [27], we calculate the expectation value of the $1/r^5$ operator for $l = 0$ atomic states to be:

$$\left\langle ns \left| \frac{1}{r^5} \right| ns \right\rangle \approx \frac{2Z^3}{n^3 r_c^2 \tilde{a}_B^3}, \quad (11)$$

where n is the principal quantum number, Z is the electric charge of the nucleus (in units of the proton electric charge e), and \tilde{a}_B is the reduced atomic Bohr radius. The cutoff parameter r_c in (11) depends on the specific system. In atoms with a hadronic nucleus, r_c is given by the nuclear radius R_{nuc} , while in exotic atoms with a non-hadronic point-like ‘‘nucleus’’, r_c is determined by the reduced Compton wavelength of the Z boson, $\lambda_Z \approx 2.16 \times 10^{-3} \text{ fm}$, which is the length scale below which the Fermi four-fermion approximation is no longer valid and the long-range potential in Eq. (1) changes to a much less singular $1/r$ form.

Positronium and muonium spectroscopy. — We first consider positronium (a bound state of an electron and a positron) and muonium (a bound state of an electron and an anti-muon). The absence of hadronic nuclei in these exotic atoms makes them very clean systems to study. Using the result (11) with $Z = 1$, we determine the energy shifts in the positronium and muonium $n {}^3S_1$ and $n {}^1S_0$ states due to the neutrino-mediated potential (1) to be:

$$\delta E(n {}^3S_1) \approx -\frac{G_F^2}{4\pi^3} \frac{2}{n^3 \lambda_Z^2 \tilde{a}_B^3} \left(a_l^2 - \frac{2}{3} b_l^2 \right), \quad (12)$$

$$\delta E(n {}^1S_0) \approx -\frac{G_F^2}{4\pi^3} \frac{2}{n^3 \lambda_Z^2 \tilde{a}_B^3} (a_l^2 + 2b_l^2), \quad (13)$$

with $\tilde{a}_B = 2a_B$ in positronium and $\tilde{a}_B \approx a_B$ in muonium.

Comparing the measured [28] and predicted [29] values of the positronium $1 {}^3S_1 - 2 {}^3S_1$ transition frequency:

$$\nu_{1S-2S}^{\text{exp}} = 1233607216.4(3.2) \text{ MHz}, \quad (14)$$

$$\nu_{1S-2S}^{\text{theor}} = 1233607222.18(58) \text{ MHz}, \quad (15)$$

and using expressions (12), (2) and (3), we place the following constraints on the neutrino-mediated potential in Eq. (1):

$$G_{\text{eff}}^2 \lesssim 1.1 \times 10^9 G_F^2. \quad (16)$$

Additionally, comparing the measured [30] and predicted [29] values of the positronium $1 {}^1S_0 - 1 {}^3S_1$ ground-state hyperfine splitting interval:

$$\nu_{\text{hfs}}^{\text{exp}} = 203389.10(74) \text{ MHz}, \quad (17)$$

$$\nu_{\text{hfs}}^{\text{theor}} = 203392.01(46) \text{ MHz}, \quad (18)$$

and using expressions (12), (13) and (3), we place the following constraints on the neutrino-mediated potential in Eq. (1):

$$G_{\text{eff}}^2 \lesssim 2.8 \times 10^7 G_F^2. \quad (19)$$

Finally, comparing the measured [31] and predicted [32, 33] values of the muonium ground-state hyperfine splitting interval:

$$\nu_{\text{hfs}}^{\text{exp}} = 4463302776(51) \text{ Hz}, \quad (20)$$

$$\nu_{\text{hfs}}^{\text{theor}} = 4463302868(271) \text{ Hz}, \quad (21)$$

and using expressions (12), (13) and (3), we place the following constraints on the neutrino-mediated potential in Eq. (1):

$$G_{\text{eff}}^2 \lesssim 3.5 \times 10^2 G_F^2. \quad (22)$$

The energy shift in the muonium ground-state hyperfine interval due to the long-range $1/r^5$ interaction mediated by pairs of standard-model neutrinos and other weakly-charged particles is at the level ≈ 1 Hz.

Hydrogen and deuterium spectroscopy. — We now consider isotope-shift spectroscopy in hydrogen and deuterium. Using the result (11) with $Z = 1$ and $\tilde{a}_B \approx a_B$, we determine the energy shifts in the hydrogen and deuterium $l = 0$ states, averaged over the respective hyperfine intervals, due to the neutrino-mediated potential (1) to be:

$$\delta E(ns) \approx \frac{G_F^2}{4\pi^3} \frac{a_l Q_W}{n^3 R_{\text{nucl}}^2 a_B^3}, \quad (23)$$

where $Q_W \equiv 2(Na_n + Za_p)$ is the weak nuclear charge, with N being the neutron number and Z the proton number.

The measured and predicted differences of the $1s - 2s$ transition frequency, averaged over the hyperfine interval, in deuterium and hydrogen are [34]:

$$\nu_{1S-2S}^{\text{D,exp}} - \nu_{1S-2S}^{\text{H,exp}} = 670994334606(15) \text{ Hz}, \quad (24)$$

$$\nu_{1S-2S}^{\text{D,theor}} - \nu_{1S-2S}^{\text{H,theor}} = 670994348.9(4.9) \text{ kHz}, \quad (25)$$

where for the predicted value, we have determined the dominant finite-nuclear-size effect using Eq. (2) of Ref. [34], together with the experimentally determined charge radii of the proton and deuteron from spectroscopy measurements in muonic hydrogen and muonic deuterium: $r_p = 0.84184(67) \text{ fm}$ [35] and $r_d = 2.12562(78) \text{ fm}$ [36]. Comparing the measured and predicted values in (24) and (25), and using expressions (23) and (2), we place the following constraints on the neutrino-mediated potential in Eq. (1):

$$G_{\text{eff}}^2 \lesssim 1.7 \times 10^{11} G_F^2. \quad (26)$$

Spectroscopy of heavy atoms. — Finally, we turn to heavy atomic species, with $Z \gg 1$. In heavy atoms, the spin-dependent terms of the potential (1) are largely ineffective, compared with the spin-independent term. The reason for this is that the spin-independent part of the potential (1) acts coherently in atoms and scales roughly with the number of neutrons $N \gg 1$, whereas the spin-dependent part acts incoherently in atoms, since ground-state nuclei have at most two unpaired nucleon spins (due to the nuclear pairing interaction).

Using the relativistic atomic wavefunctions for a valence electron at small distances [37] (where the Coulomb field of the nucleus is unscreened), we calculate the expectation value of the operator (1), due to neutrino-pair exchange between atomic electrons and nucleons, for an atomic single-particle state with total angular momentum $j = 1/2$ to be:

$$\delta E_\kappa \approx \frac{G_F^2}{4\pi^3} \frac{[(\kappa - \gamma)^2 + (Z\alpha^2)]Z(Z_i + 1)^2}{(2 - \gamma)\nu^3 R_{\text{nucl}}^2 a_B^3} \times \frac{a_l Q_W}{[\Gamma(2\gamma + 1)]^2} \left(\frac{a_B}{2ZR_{\text{nucl}}} \right)^{2-2\gamma}, \quad (27)$$

where $\kappa = (-1)^{l-1}$, $\gamma = \sqrt{1 - (Z\alpha)^2}$, $\alpha \approx 1/137$ is the electromagnetic fine-structure constant, Z_i is the

net charge of the atomic species (for a neutral atom $Z_i = 0$), and ν is the effective principal quantum number, defined via the ionisation energy of the valence electron: $I = m_e \alpha^2 (Z_i + 1)^2 / (2\nu^2)$. In heavy nuclei, the nuclear radius is generally well described by the relation $R_{\text{nucl}} = A^{1/3} r_0$, where $A = Z + N$ is the nucleon number and $r_0 \approx 1.2 \text{ fm}$.

To estimate the contribution of neutrino-pair exchange between atomic electrons to the energy shift in heavy atoms, we note that in this case the valence atomic electrons now interact predominantly with a ‘core’ of two $1s$ electrons (which are situated mainly at the distances $r \sim r_{1s} = a_B/Z$), instead of mainly with the N neutrons of the nucleus. Thus the electron-electron contribution to the energy shift in heavy atoms is parametrically suppressed compared to the electron-nucleon contribution by the factor $(R_{\text{nucl}}/r_{1s})^2/N \ll 1$.

Calcium-ion isotope-shift spectroscopy and non-linearities of the King plot. — Many-electron atomic systems function as the most precise systems in metrology, with optical atomic and ionic clocks already demonstrating a fractional precision at the level of $\sim 10^{-18}$ [14–19]. At the same time, the complexity of many-electron atoms means that theoretically predicted values for transition frequencies in these systems generally have a precision that is many orders of magnitude worse than the corresponding experimental precision. To circumvent this issue, one can utilise isotope-shift measurements in atoms and look for non-linearities in the King plot [38], a technique which was recently considered in Refs. [39–42] in the different context of probing Yukawa interactions of hypothetical Higgs-like particles.

As a specific example, we consider isotope-shift spectroscopy measurements in Ca^+ ($Z = 20$, $Z_i = 1$). Ca^+ is an excellent system for isotope-shift spectroscopy, since it has five stable or long-lived isotopes with spinless nuclei ($A = 40, 42, 44, 46, 48$), as well as several readily accessible optical transitions [43, 44]. We shall consider the pair of transitions, ${}^2S_{1/2} - {}^2P_{1/2}$ and ${}^2D_{3/2} - {}^2P_{1/2}$, to which we refer as transitions 1 and 2, respectively. In this case, the dominant effect of the neutrino-mediated potential (1) is on the S -level in transition 1, see Eq. (27). We can thus write the differences in the transition frequency between two isotopes A and A' , $\nu_i^{AA'} = \nu_i^A - \nu_i^{A'}$, for the two transitions in the following form:

$$\nu_1^{AA'} \approx K_1 \mu_{AA'} + F_1 \delta \langle r^2 \rangle_{AA'} - \delta E_{\kappa=-1}^{AA'}, \quad (28)$$

$$\nu_2^{AA'} \approx K_2 \mu_{AA'} + F_2 \delta \langle r^2 \rangle_{AA'}, \quad (29)$$

where K_i and F_i are the usual mass-shift and field-shift parameters, $\mu_{AA'} = 1/m_A - 1/m_{A'}$, with m_A and $m_{A'}$ being the respective masses of isotopes A and A' , and $\delta E_{\kappa=-1}^{AA'} = \delta E_{\kappa=-1}^A - \delta E_{\kappa=-1}^{A'}$ is the difference of the neutrino-induced S -level energy shift between the two isotopes A and A' . Dividing Eqs. (28) and (29) by $\mu_{AA'}$, and simultaneously solving the resulting equations, we can eliminate the difference in the square of the charge

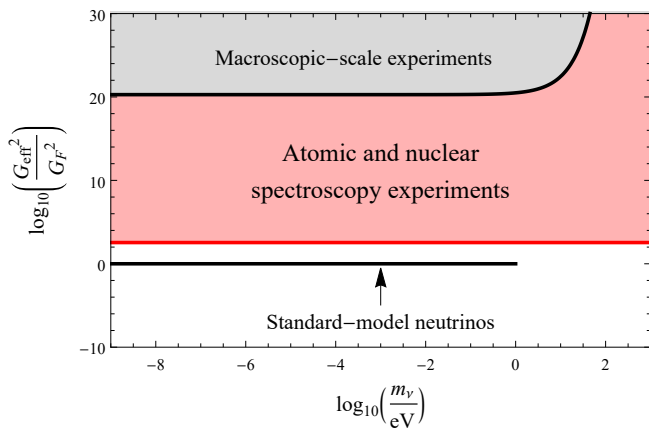


FIG. 2. (Color online) Limits on the neutrino-mediated potential in Eq. (1), as a function of the neutrino mass m_ν . The red region represents constraints derived in the present work from atomic and nuclear spectroscopy. The grey region represents constraints from experiments that search for new macroscopic forces [9–13]. The black line with $G_{\text{eff}} = G_{\text{F}}$ corresponds to the strength of forces mediated by neutrinos and other weakly-charged particles in the standard model.

radii between the two isotopes, $\delta \langle r^2 \rangle_{AA'}$, to give the following equation in terms of the modified frequencies $M\nu_i^{AA'} = \nu_i^{AA'}/\mu_{AA'}$:

$$M\nu_1^{AA'} = K_{12} + F_{12}M\nu_2^{AA'} - \frac{\delta E_{\kappa=-1}^{AA'}}{\mu_{AA'}}, \quad (30)$$

where $K_{12} = K_1 - F_{12}K_2$ and $F_{12} = F_1/F_2$.

We see that the last term on the right-hand side of

Eq. (30) scales as $\propto AA'$ and thus gives rise to a non-linearity in the plot of $M\nu_1^{AA'}$ versus $M\nu_2^{AA'}$ (the so-called King plot [38]). Such non-linearities have been constrained experimentally at the level $\lesssim 25 \text{ MHz} \cdot \text{GeV}$ over the interval $40 \leq A \leq 48$ [43]. We can use this experimental result, together with expressions (27) and (2), to constrain the neutrino-mediated potential in Eq. (1). For the input parameters of (27), we use the measured value of the ionisation energy of the $^2S_{1/2}$ state in Ca^+ : $I \approx 11.9 \text{ eV}$ [45], and, since the measured differences in the mean-square nuclear charge radii are relatively small across all of the relevant Ca^+ isotopes [43], for simplicity we can assume the nuclear radius $R_{\text{nucl}} = A^{1/3}r_0$ with $A = 44$ for all of the relevant isotopes. This yields the following constraint:

$$G_{\text{eff}}^2 \lesssim 4.1 \times 10^{11} G_{\text{F}}^2. \quad (31)$$

Conclusions. — We have calculated the effects of the neutrino-mediated potential in Eq. (1) on transition and binding energies in atoms and nuclei. Using existing spectroscopic data, we have derived constraints on neutrino-mediated forces (see Fig. 2). Our derived limits improve on existing constraints on neutrino-mediated forces from experiments that search for new spin-independent [9–11] and spin-dependent [12, 13] macroscopic forces by 18 orders of magnitude. Future spectroscopy experiments have the potential to probe long-range forces mediated by the exchange of pairs of standard-model neutrinos and other weakly-charged particles.

Acknowledgements. — I am grateful to Victor Flambaum for helpful discussions. This work was supported by the Humboldt Research Fellowship.

-
- [1] C. Patrignani *et al.* (Particle Data Group), *Chin. Phys. C* **40**, 100001 (2016).
- [2] L. M. Brown and H. Rechenberg, *The origin of the concept of nuclear forces*, Institute of Physics Publishing, Bristol, 1996.
- [3] G. Feinberg and J. Sucher, *Phys. Rev.* **166**, 1638 (1968).
- [4] G. Feinberg, J. Sucher, C.-K. Au, *Phys. Rept.* **180**, 83 (1989).
- [5] S. D. H. Hsu and P. Sikivie, *Phys. Rev. D* **49**, 4951 (1994).
- [6] J. A. Grifols, E. Masso, R. Toldra, *Phys. Lett. B* **389**, 563 (1996).
- [7] F. Ferrer, J. A. Grifols, M. Nowakowski, *Phys. Lett. B* **446**, 111 (1999).
- [8] V. V. Flambaum and E. V. Shuryak, *Phys. Rev. C* **76**, 065206 (2007).
- [9] D. J. Kapner, T. S. Cook, E. G. Adelberger, J. H. Gundlach, B. R. Heckel, C. D. Hoyle, H. E. Swanson, *Phys. Rev. Lett.* **98**, 021101 (2007).
- [10] E. G. Adelberger, B. R. Heckel, S. Hoedl, C. D. Hoyle, D. J. Kapner, A. Upadhye, *Phys. Rev. Lett.* **98**, 131104 (2007).
- [11] Y.-J. Chen, W. K. Tham, D. E. Krause, D. Lopez, E. Fischbach, R. S. Decca, *Phys. Rev. Lett.* **116**, 221102 (2016).
- [12] G. Vasilakis, J. M. Brown, T. W. Kornack, M. V. Romalis, *Phys. Rev. Lett.* **103**, 261801 (2009).
- [13] W. A. Terrano, E. G. Adelberger, J. G. Lee, B. R. Heckel, *Phys. Rev. Lett.* **115**, 201801 (2015).
- [14] C. W. Chou, D. B. Hume, J. C. J. Koelemeij, D. J. Wineland, T. Rosenband, *Phys. Rev. Lett.* **104**, 070802 (2010).
- [15] N. Hinkley, J. A. Sherman, N. B. Phillips, M. Schioppo, N. D. Lemke, K. Beloy, M. Pizzocaro, C. W. Oates, A. D. Ludlow, *Science* **341**, 1215 (2013).
- [16] B. J. Bloom, T. L. Nicholson, J. R. Williams, S. L. Campbell, M. Bishof, X. Zhang, W. Zhang, S. L. Bromley, J. Ye, *Nature* **506**, 71 (2014).
- [17] I. Ushijima, M. Takamoto, M. Das, T. Ohkubo, H. Katori, *Nature Photonics* **9**, 185 (2015).
- [18] T. L. Nicholson *et al.*, *Nat. Comm.* **6**, 6896 (2015).
- [19] N. Huntemann, C. Sanner, B. Lipphardt, Chr. Tamm, E. Peik, *Phys. Rev. Lett.* **116**, 063001 (2016).
- [20] Ch. Kraus *et al.*, *Eur. Phys. J. C* **40**, 447 (2005).

- [21] V. N. Aseev *et al.*, Phys. Rev. D **84**, 112003 (2011).
- [22] The effects of the running of the Weinberg angle parameter $\sin^2(\theta_W)$ are relatively small for the momentum scales that are relevant in the present work [23], so we assume the constant value $\sin^2(\theta_W) \approx 0.24$.
- [23] A. Czarnecki and W. J. Marciano, Int. J. Mod. Phys. A **15**, 2365 (2000).
- [24] E. G. Kessler, Jr., M. S. Dewey, R. D. Deslattes, A. Henins, H. G. Boerner, M. Jentschel, C. Doll, H. Lehmann, Phys. Lett. A **255**, 221 (1999).
- [25] D. R. Entem, R. Machleidt, Phys. Rev. C **68**, 041001(R) (2003).
- [26] A. Ekstroem, G. R. Jansen, K. A. Wendt, G. Hagen, T. Papenbrock, B. D. Carlsson, C. Forssen, M. Hjorth-Jensen, P. Navratil, W. Nazarewicz, Phys. Rev. C **91**, 051301(R) (2015).
- [27] L. D. Landau and E. M. Lifshitz, *Quantum Mechanics (Nonrelativistic Theory)*, 3rd ed. (Butterworth-Heinemann, Oxford, 1977).
- [28] M. S. Fee, A. P. Mills, Jr., S. Chu, E. D. Shaw, K. Danzmann, R. J. Chichester, D. M. Zuckerman, Phys. Rev. Lett. **70**, 1397 (1993).
- [29] A. Czarnecki, K. Melnikov, A. Yelkhovskiy, Phys. Rev. A **59**, 4316 (1999).
- [30] M. W. Ritter, P. O. Egan, V. W. Hughes, K. A. Woodle, Phys. Rev. A **30**, 1331 (1984).
- [31] W. Liu *et al.*, Phys. Rev. Lett. **82**, 711 (1999).
- [32] A. Czarnecki, S. I. Eidelman, S. G. Karshenboim, Phys. Rev. D **65**, 053004 (2002).
- [33] P. J. Mohr, D. B. Newell, B. N. Taylor, Rev. Mod. Phys. **88**, 035009 (2016).
- [34] C. G. Parthey, A. Matveev, J. Alnis, R. Pohl, T. Udem, U. D. Jentschura, N. Kolachevsky, T. W. Haensch, Phys. Rev. Lett. **104**, 233001 (2010).
- [35] R. Pohl *et al.*, Nature **466**, 213 (2010).
- [36] R. Pohl *et al.*, Science **353**, 669 (2016).
- [37] I. B. Khriplovich, *Parity Nonconservation in Atomic Phenomena*, Gordon and Breach, Philadelphia, 1991.
- [38] W. H. King, J. Opt. Soc. Am. **53**, 638 (1963).
- [39] C. Delaunay, R. Ozeri, G. Perez, Y. Soreq, arXiv:1601.05087.
- [40] C. Frugiuele, E. Fuchs, G. Perez, M. Schlaffer, Phys. Rev. D **96**, 015011 (2017).
- [41] J. C. Berengut *et al.*, arXiv:1704.05068.
- [42] V. V. Flambaum, A. J. Geddes, A. V. Viatkina, arXiv:1709.00600.
- [43] F. Gebert, Y. Wan, F. Wolf, C. N. Angstmann, J. C. Berengut, P. O. Schmidt, Phys. Rev. Lett. **115**, 053003 (2015).
- [44] C. Shi *et al.*, Appl. Phys. B **123**, 2 (2017).
- [45] *NIST Atomic Spectra Database Ionization Energies Form*, National Institute of Standards and Technology, <https://physics.nist.gov/PhysRefData/ASD/ionEnergy.html>